

Electromechanical control of quantum emitters in nanophotonic devices

B. Machielse^{1*}, S. Bogdanovic^{2*}, S. Meesala^{2*}, S. Gauthier³, M. J. Burek², G. Joe², M. Chalupnik¹, Y. I. Sohn², J. Holzgrafe², R. E. Evans¹, C. Chia², H. Atikian², M. K. Bhaskar¹, D. D. Sukachev^{1,4}, L. Shao², S. Maity², M. D. Lukin¹, M. Loncar²

¹ Department of Physics, Harvard University, Cambridge, MA 02138, USA

² John A. Paulson School of Engineering and Applied Sciences, Harvard University, Cambridge, MA 02138, USA

³ Department of Physics and Astronomy, University of Waterloo, 200 University Avenue West
Waterloo, Ontario, Canada

⁴ P. N. Lebedev Physical Institute of the RAS, Moscow 119991, Russia

* These authors contributed equally to this work

† Corresponding author. Email: loncar@seas.harvard.edu

Photon-mediated coupling between distant matter qubits [1,2] may enable secure communication over long distances, the implementation of distributed quantum computing schemes, and the exploration of new regimes of many-body quantum dynamics [3,4]. Nanophotonic devices coupled to solid-state quantum emitters represent a promising approach towards realization of these goals, as they combine strong light-matter interaction and high photon collection efficiencies [5-7]. However, the scalability of these approaches is limited by the frequency mismatch between solid-state emitters and the instability of their optical transitions [7]. Here we present a nano-electromechanical platform for stabilization and tuning of optical transitions of silicon-vacancy (SiV) color centers in diamond nanophotonic devices by dynamically controlling their strain environments. This strain-based tuning scheme has sufficient range and bandwidth to alleviate the spectral mismatch between individual SiV centers. Using strain, we ensure overlap between color center optical transitions and observe an entangled superradiant state by measuring correlations of photons collected from the diamond waveguide. This platform for tuning spectrally stable color centers in nanophotonic waveguides and resonators constitutes an important step towards a scalable quantum network.

Solid-state emitters with inversion symmetry [8] are promising for use in quantum networking protocols due to their ability to be integrated into nanophotonic devices [9-11]. These emitters have suppressed static electric dipole moments, increasing the stability of their optical transition frequencies to fluctuations of electric fields that occur near device surfaces [8,12]. The negatively charged silicon vacancy center (SiV) in diamond nanophotonic devices is the most mature among the platforms leveraging this property. The SiV features enhanced emitter-photon interactions with cooperativity greater than 20 in nanophotonic cavities [11], as well as all other essential components for quantum networking, such as a long-lived quantum memory [10] and efficient photon collection [13].

However, the technological applicability of these emitters is still limited by the substantial inhomogeneous distributions of their optical transition frequencies as well as the residual instability in the form of spectral diffusion [8, 12]. Demonstrating full control of their spectral properties is an essential requirement for their implementation in scalable quantum networks [14]. Because these emitters cannot be spectrally tuned using electric fields—the established tuning mechanism for solid-state emitters [7, 15]—previous attempts to enable spectral overlap have relied on Raman [9, 16] and magnetic field [11] tuning. However, these techniques constrain either the spin or optical degree of freedom of the color center and are challenging to implement beyond the few-qubit regime.

Inspired by experiments involving semiconductor quantum dots [17,18], initial experiments with diamond cantilevers have demonstrated the capacity to tune individual, free space coupled SiV center optical transition frequencies using strain [19, 20]. It remains an outstanding challenge to develop a scalable implementation of strain tunable emitters coupled to nanophotonic devices.

Here we present a diamond platform that combines nano-electromechanical system (NEMS) and nanophotonic technology to strain-tune SiV color centers and stabilize their optical transition frequencies. Using this technology, we observe a superradiant, entangled state between strain-tuned, waveguide-coupled SiV centers; this showcases strain tuning as an important tool for ensuring indistinguishability between SiV center qubits in a multi-node quantum network.

Our approach utilizes nanophotonic devices (Figure 1) that consist of triangular cross-section waveguides fabricated from single crystal diamond using an angled ion beam etching technique (Figure S1) [21, 22]. Each of these waveguides is connected to a support structure on one end (Figure 1b) with the other end tapered to allow for 85% efficiency photon collection into an optical fiber (Figure 1c) [13].

In order to embed SiV centers within diamond nanophotonic devices, we adapt a masked implantation technique previously used for bulk substrates [23, S1]. After the creation of SiV centers, gold electrodes are patterned onto the devices such that metallized parts of the waveguide act as one plate of a capacitor, with the other plate located on the diamond substrate (Figure 1b). Applying a voltage difference to these plates generates a force that deflects a portion of the waveguide, applying electrically controllable strain to the embedded SiV centers.

We measure the strain response of two SiV centers 30 μm apart within the same diamond photonic device via resonant excitation of their optical transitions and collection of their phonon sideband emission (Figure 2). The difference in the position of SiV centers in the device accounts for the difference in their response to the applied voltage [20], allowing us to overlap their optical transitions (Figure 2, red inset). We observe a tuning range of over 80 GHz, a factor of 3 larger than the total inhomogeneous distribution of the SiV optical transitions measured in these devices (blue shaded regions of Figure 2).

To determine the bandwidth of our electromechanical actuation scheme, we investigate an SiV color center's spectral response to AC mechanical driving of the nanophotonic structure (Figure

2, inset). We apply a DC bias combined with a variable-frequency RF signal to the gold electrodes and monitor the SiV optical transition. When the RF drive frequency matches one of the nanobeam's mechanical modes, we observe linewidth broadening of the SiV coupled to this mechanical mode [25]. Using this technique, we observe modes with mechanical frequencies of up to 100 MHz. Optimizing the device design could enable the electromechanical driving of GHz frequency vibrational modes resonant with SiV spin transitions, and thereby open new possibilities for engineering coherent spin-phonon interactions [19].

The high bandwidth of our electromechanical actuation scheme is sufficient to suppress spectral diffusion exhibited by the SiV center [12]. Monitoring an SiV center's optical transition over the course of five hours, we observe spectral diffusion that is an order of magnitude larger compared to its single-scan linewidth of around 300 MHz (Figure 3a). We use electromechanical control over the local strain field to correct for slow spectral diffusion [18]. Using a pulsed feedback scheme that applies a voltage adjustment every 20 seconds, limited by the duration of the broad laser scan [SI], we reduce the total summed linewidth by almost an order of magnitude on a timescale of several hours (Figure 3b).

We monitor the noise spectrum of the SiV center emission with and without a 5 Hz lock-in feedback scheme applied to the device voltage. The application of feedback results in an intensity noise reduction of approximately 8 dB (Figure 3c). We attribute the frequency component dominated by the $1/f$ noise to slow strain fluctuations and second order susceptibility to electric field fluctuations in the SiV environment. Beyond this regime, our feedback scheme is limited by photon shot noise. Further improving the SiV count rate through Purcell enhancement using a cavity could enable higher frequency locking of SiV spectral lines to an arbitrary frequency standard, as the existing feedback scheme uses only a small share of the available actuation bandwidth.

With the optical transitions of the SiV centers tuned and stabilized, we proceed to generate probabilistic entanglement between two color centers. We start by using strain control to set the optical transition frequencies between the lower branch of the ground state ($|c\rangle$) and the excited state ($|e\rangle$) of two emitters at the target detuning (Δ) by applying the appropriate voltage (Figure 4a). The transitions between the upper branch of the ground state ($|u\rangle$) and the excited state ($|e\rangle$) of the two emitters are then continuously excited using two separate lasers (Figure 4a). Finally, the photons emitted into the diamond waveguide are collected through a tapered fiber interface and filtered using a high finesse Fabry-Perot filter [SI] in order to separate the desired optical transition from the excitation laser [9]. We characterize our setup by measuring the second order correlation function in case of a single emitter (Figure 4c, gray path) and two distinguishable emitters ($\Delta \neq 0$, Figure 4c, blue path) observing $g^{(2)}_{\text{single}}(0) = 0.13(4)$ and $g^{(2)}_{\text{dist}}(0) = 0.50(7)$ respectively, in good agreement with the theory [SI].

When the two SiV optical transitions are tuned into resonance ($\Delta = 0$), detection of the first emitted photon from a pair of excited SiV color centers projects the system into an entangled, bright state (Figure 4b, red path). This state is identified by the superradiant emission of a second

photon at twice the rate expected from the distinguishable case [9, 26]. We confirm the generation of an entangled state by observing a superradiant peak in the photon correlation function (Figure 4c, right panel) with $g^{(2)}_{\text{ind}}(0) = 0.88(8)$. Experimental results are in good agreement with a simulated model of our system (Figure 4c, red curve) which uses only a single fitting parameter [27, SI]. Using the height of the superradiant peak and the value of the $g^{(2)}_{\text{single}}$, we calculate a lower bound on the conditional bright state fidelity of 0.8(1) [9], indicating the observation of a probabilistically-generated entangled state (Figure S3).

These observations demonstrate the potential of the developed strain tuning technique to enable optically mediated interactions between spatially separated emitters. A strain-tunable, solid-state emitter strongly coupled to a nanophotonic cavity could represent an important component of a scalable quantum network. We note that current experiments using diamond photonic crystals rely on a diamond waveguide perforated with an array of holes [9, 12, 13, 21, 22], where the fundamental optical mode has poor overlap with the strain field induced when the device is deflected (Figure 5a).

Dramatic improvement in the overlap between the optical and strain fields could be achieved by transitioning to a “ribbed” cavity design [28], where the unit cell is defined by a thin central waveguide structure with external corrugation (Figure 5b, inset). A suitable SiV implantation spot (Figure 5b, red circle) would allow for the tuning of implanted SiV centers by an average of more than 50 GHz. Using finite-difference time-domain simulations, we developed an optimized cavity design with simulated Q of greater than 25,000 and mode volume of $1.21 (\lambda/n)^3$. We estimate that a cooperativity $C > 6$ could be achieved in such ribbed cavities [SI].

Furthermore, by implanting a fraction of the color centers in regions of the cavity with low strain but high optical field intensity, SiV centers coupled to the same cavity could be tuned relative to each other. This could make it possible to rapidly modulate their cavity-mediated interactions, a potential basis for designing multiqubit registers in single quantum network nodes [12, 29].

We have presented a platform for the direct tuning and stabilization of SiV optical transitions within nanophotonic devices. We demonstrated a reduction of spectral diffusion by almost an order of magnitude over a broad bandwidth and achieved a spectral tuning range exceeding 150 pm, several times greater than the SiV inhomogeneous distribution. Using this method of SiV center spectral control, we have observed an optically mediated entangled state between two SiV centers located within the same diamond waveguide. Together, these demonstrations show that strain can be used to overcome the limits on resonant interaction of SiV centers imposed by spectral mismatch and diffusion. Furthermore, this approach can be directly adapted to quantum dots, as well as other inversion-symmetric color centers in diamond [30] and other materials. This integration of strain tuning technology with nanophotonic cavities provides a promising route towards creation of integrated quantum nodes, paving the way for the realization of a scalable quantum network.

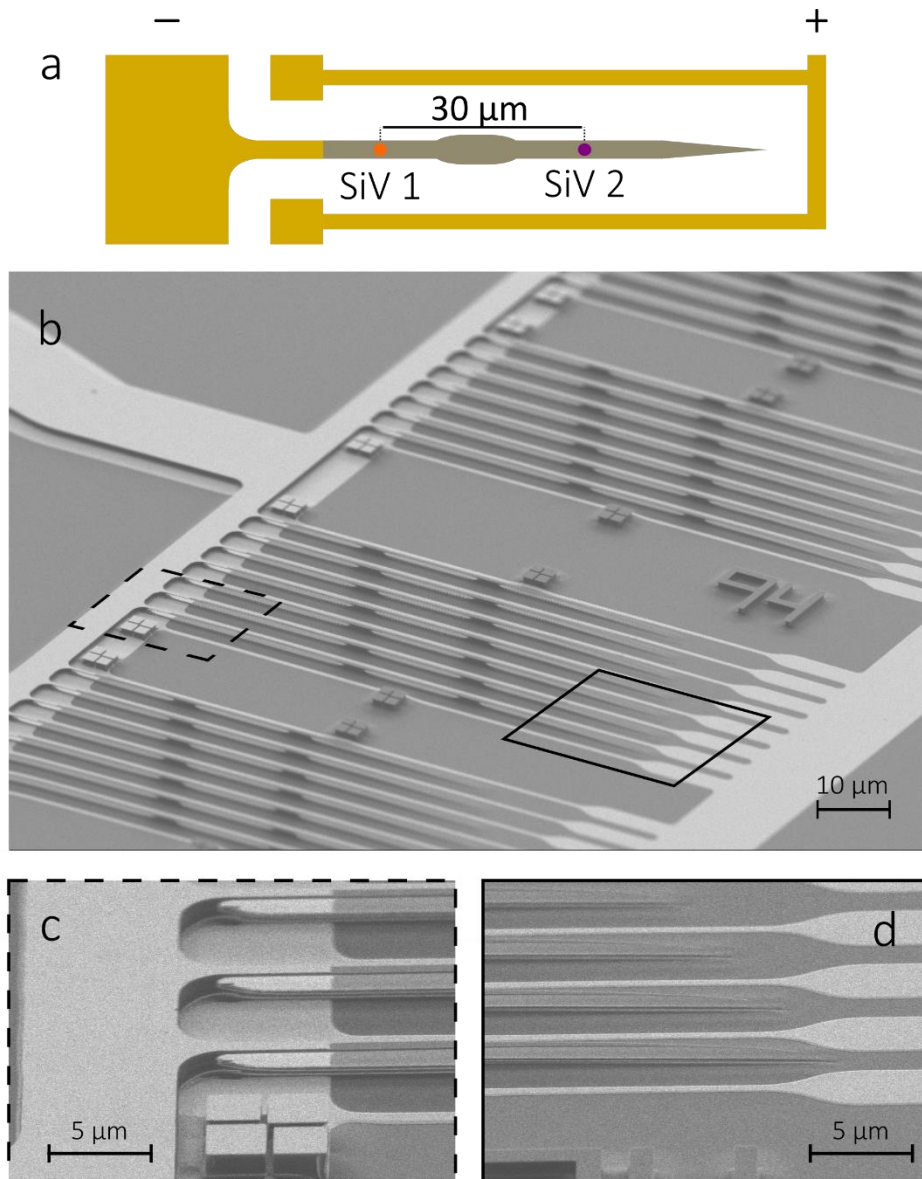


Figure 1: Schematic of diamond nanophotonics device. a) Diamond waveguides (gray) are implanted with color centers (purple and orange) at desired locations on the device. Electrodes (gold) are used to define a capacitor between plates located on the device (negative terminal) and below the device (positive terminal). Applying bias voltage between the plates causes the deflection of the doubly clamped cantilever. This tunes color centers between the plates and the first clamp (orange spot) without perturbing color centers beyond the clamp (purple spot). **b)** Scanning electron micrograph (SEM) of the photonic devices. **c)** Capacitor plates located on and below the devices. **d)** Diamond tapers used to extract photons from waveguides. This enables the extraction efficiency of more than 85% from the diamond waveguide into the fiber.

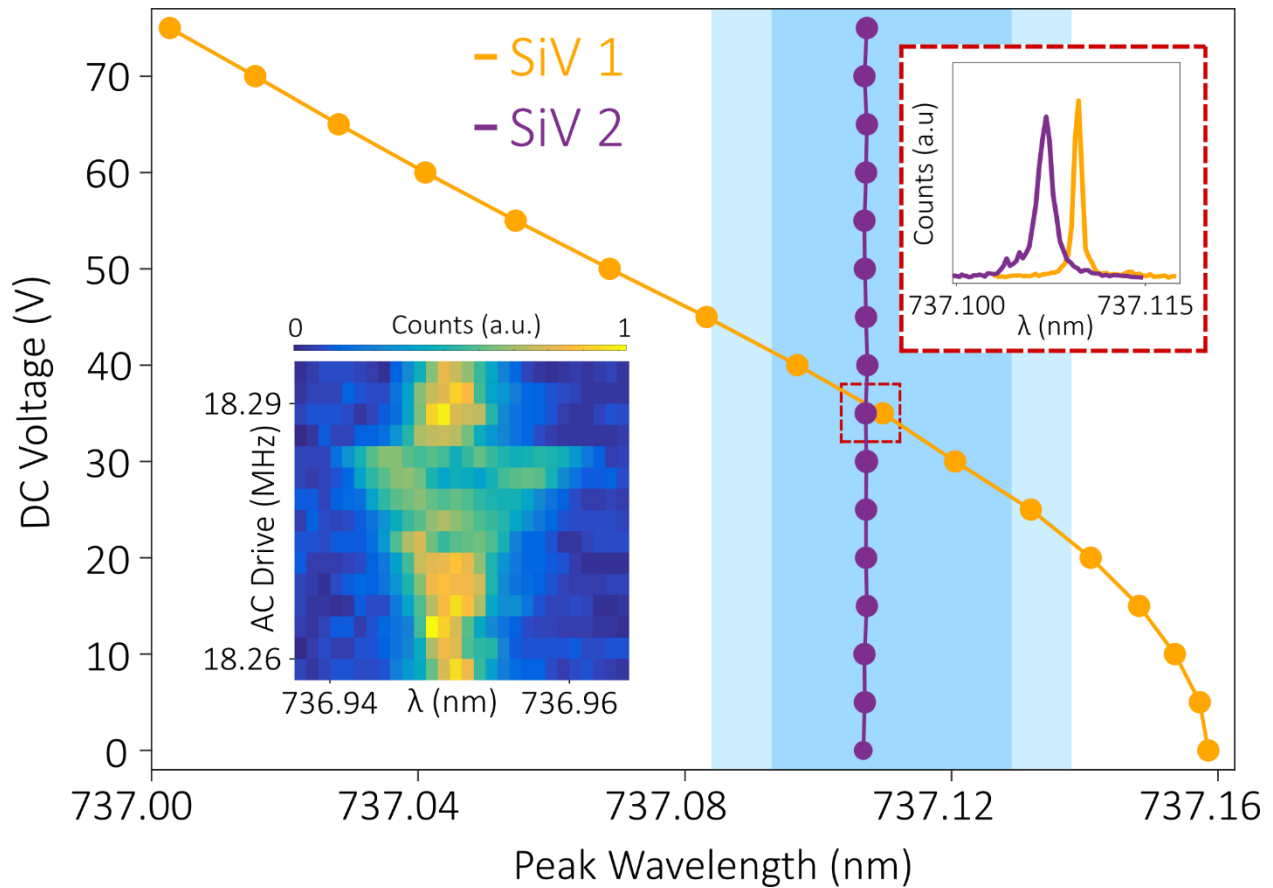


Figure 2: Characterization of DC and AC voltage response of the devices. Voltage bias is applied to the capacitor plates, resulting in strain fields that tune the optical transitions of SiV1 in the deflected portion of the device (orange) compared to the optical transitions of SiV2 in the stationary regions (purple). The tuning range of the SiV color center greatly exceeds the inhomogeneous distribution for 50% (75%) of SiV color centers observed in this experiment shown in dark (light) blue shading. The red inset shows the photoluminescence excitation spectra of two color centers at a voltage near the overlap. The blue inset shows the AC response of the cantilever system, measured by observing SiV optical transitions while modulating the AC driving frequency. Driving the cantilever resonance with its mechanical mode results in linewidth broadening of the color center optical transitions.

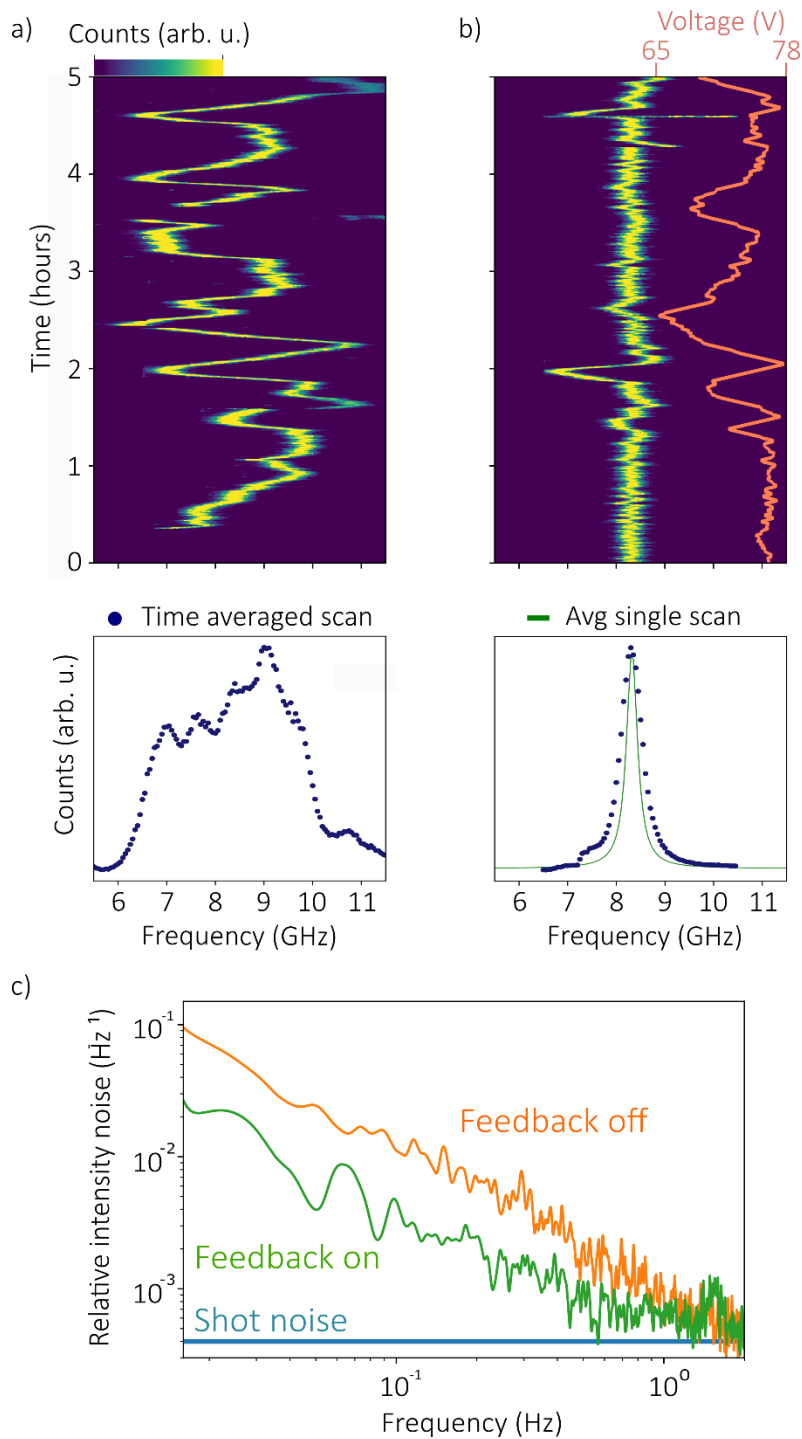


Figure 3: Reduction of spectral diffusion using nanomechanical strain. a) Top: Spectral diffusion of SiV center optical transition, measured over a 5-hour period. Bottom: Time-averaged spectrum over the same period. **b)** Top: Measurement of the SiV spectral diffusion with 20 second pulsed feedback over a 5-hour period. Bottom: Time-averaged spectra over a 5-hour period (blue dots) show the reduction of total linewidth down to 500 MHz. The average of single-scan SiV linewidths is 350 MHz (green line). **c)** PSD of measured SiV count fluctuations with (without) feedback is presented by the green (orange) line, showing reduction of noise by an average of 8 dB. Blue line indicates statistical noise limit set by finite photon emission and collection rate.

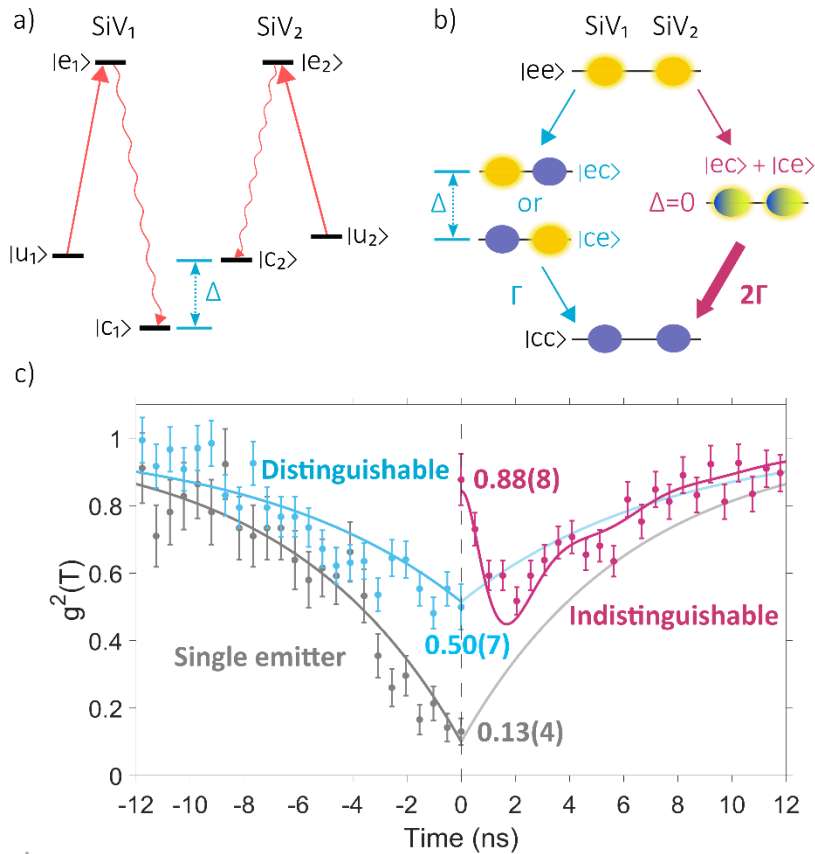


Figure 4: Generation of the superradiant entangled state using strain control. a) Level structure for two SiV centers. Separate lasers are applied to excite the $|u\rangle$ to $|e\rangle$ transition of each emitter. Strain tuning of one SiV color center changes the detuning (Δ) between their $|e\rangle$ to $|c\rangle$ transitions. Photons resulting from the decay from $|e\rangle$ to $|c\rangle$ are collected through the diamond waveguide. **b)** A single photon emitted from the two excited emitters with distinguishable transitions ($\Delta \neq 0$) projects the system to a statistical mixture of $|ec\rangle$ and $|ce\rangle$ states (blue decay path). When the emitters are indistinguishable ($\Delta = 0$), the emission of one photon projects the system into a superradiant bright state (purple decay path) that decays at a rate two times faster than that of the statistical mixture. **c)** The second order photon correlation function is measured for a single emitter (left panel, gray data points) and for two spectrally distinguishable emitters (left panel, blue data points). Measured $g^{(2)}(0)$ is 0.13(4) and 0.50(7) for the single emitter and distinguishable cases, respectively. Exponential curves fit to the data are plotted and mirrored onto the right half of plot (gray and blue lines). For two emitters tuned into resonance, we observe the generation of a superradiant entangled state, signified by the peak in the photon correlation (right panel, purple data points). Data is overlaid with a simulated model with a single fit parameter [SI]. For indistinguishable emitters, we measure $g^{(2)}(0)=0.88(8)$, limited primarily by detector jitter.

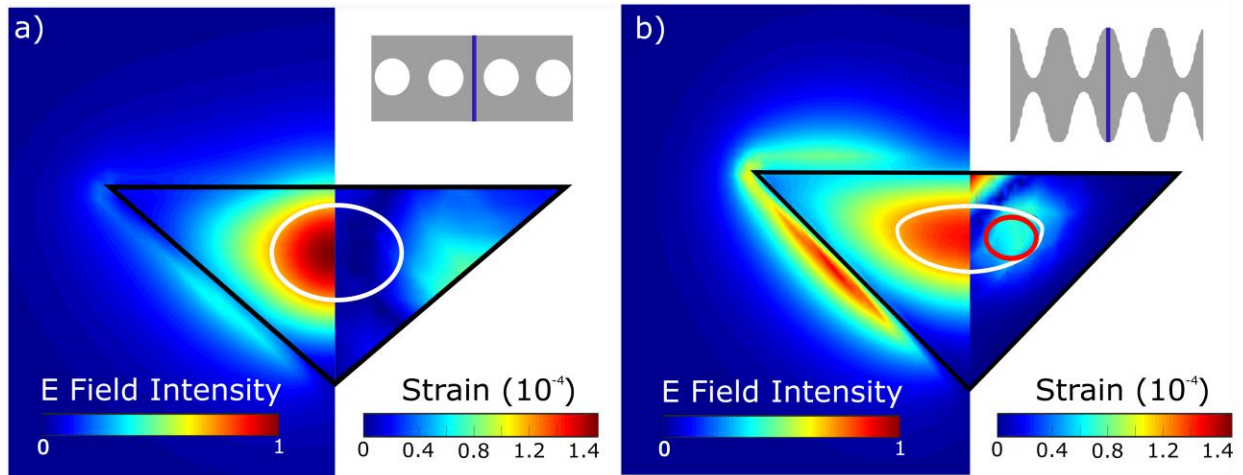


Figure 5: Scheme for strain tuning SiV color centers inside photonic crystal cavities. a) Optical (left) and strain (right) fields inside perforated photonic crystal cavities (inset). Blue line in inset represents cross section shown in electric field and strain plots. Strain is measured along one of the TE-oriented SiV axis. White contour indicates region with optical field intensity greater than 70%. Perforated structure requires compromising either optical or strain field intensity at color center position. **b)** Optical and strain fields inside ribbed cavity (inset) with simulated quality factor $Q > 25,000$. White contour indicates the region with optical field intensity greater than 70%. Red circle indicates potential SiV implantation spot with optimized optical and strain field coupling.

1. Briegel, H. J., et al. (1998). "Quantum Repeaters: The Role of Imperfect Local Operations in Quantum Communication." Physical Review Letters **81**(26): 5932-5935.
2. Duan, L. M., et al. (2001). "Long-distance quantum communication with atomic ensembles and linear optics." Nature **414**: 413.
3. Kimble, H. J. (2008). "The quantum internet." Nature **453**(7198): 1023-1030.
4. Wehner, S., et al. (2018). "Quantum internet: A vision for the road ahead." Science **362**(6412): eaam9288.
5. Hucul, D., et al. (2014). "Modular entanglement of atomic qubits using photons and phonons." Nature Physics **11**: 37.
6. Stockill, R., et al., (2017). "Phase-Tuned Entangled State Generation between Distant Spin Qubits." Physical Review Letters **119**, 010503
7. Gao, W. B., et al. (2015). "Coherent manipulation, measurement and entanglement of individual solid-state spins using optical fields." Nature Photonics **9**: 363.
8. Hepp, C., et al. (2014). "Electronic Structure of the Silicon Vacancy Color Center in Diamond." Physical Review Letters **112**(3): 036405
9. Sipahigil, A., et al. (2016). "An integrated diamond nanophotonics platform for quantum-optical networks." Science **354**(6314): 847-850.
10. Sukachev, D. D., et al. (2017). "Silicon-Vacancy Spin Qubit in Diamond: A Quantum Memory Exceeding 10 ms with Single-Shot State Readout." Physical Review Letters **119**(22): 223602.
11. Evans, R. E., et al. (2018). "Photon-mediated interactions between quantum emitters in a diamond nanocavity." Science **362**(6415): 662-665.
12. Evans, R.E., et al (2016) "Narrow-Linewidth Homogeneous Optical Emitters in Diamond Nanostructures via Silicon Ion Implantation" Phys. Rev. Applied **5**, 044010
13. Burek, M. J., et al. (2017). "Fiber-Coupled Diamond Quantum Nanophotonic Interface." Physical Review Applied **8**(2): 024026.
14. Lodahl, P. (2018). "Scaling up solid-state quantum photonics." Science **362**(6415): 646.
15. Tamarat, P., et al. (2006). "Stark Shift Control of Single Optical Centers in Diamond." Physical Review Letters **97**(8): 083002.
16. Sun, S., et al. (2018). "Cavity-Enhanced Raman Emission from a Single Color Center in a Solid." Phys Rev Lett **121**(8): 083601.
17. Sun, S., et al. (2013). "Strain tuning of a quantum dot strongly coupled to a photonic crystal cavity." Applied Physics Letters **103**(15): 151102.
18. Zopf, M., et al. (2018). "Frequency feedback for two-photon interference from separate quantum dots." Physical Review B **98**(16): 161302.
19. Meesala, S., et al. (2018). "Strain engineering of the silicon-vacancy center in diamond." Physical Review B **97**(20): 205444.
20. Sohn, Y. I., et al. (2018). "Controlling the coherence of a diamond spin qubit through its strain environment." Nat Commun **9**(1): 2012.
21. Burek, M. J., et al. (2014). "High quality-factor optical nanocavities in bulk single-crystal diamond." Nat Commun **5**: 5718.
22. Atikian, H. A., et al. (2017). "Freestanding nanostructures via reactive ion beam angled etching." APL Photonics **2**(5): 051301.
23. Toyli, D. M., et al. (2010). "Chip-Scale Nanofabrication of Single Spins and Spin Arrays in Diamond." Nano Letters **10**(8): 3168-3172.
24. Schroder, T., et al. (2017). "Scalable focused ion beam creation of nearly lifetime-limited single quantum emitters in diamond nanostructures." Nat Commun **8**: 15376.
25. P. Ouartchayapong, et al. (2014). "Dynamic strain-mediated coupling of a single diamond spin to a mechanical resonator." Nat Commun **5**: 4429 (2014).

26. Gross, M. and Haroche, S. (1982). "Superradiance: An essay on the theory of collective spontaneous emission" Phys. Reports, **93**(5) 301-396
27. Johansson, J. R., et al. (2013). "QuTiP 2: A Python framework for the dynamics of open quantum systems.", Comp. Phys. Comm. **184**, 1234
28. Zhong, T., et al. (2018). "Optically Addressing Single Rare-Earth Ions in a Nanophotonic Cavity" Physical Review Letters **121**, 183603
29. Majer, J., et al. (2007) "Coupling superconducting qubits via a cavity bus" Nature **449**, 443–447
30. Maity, S., et al. (2018). "Spectral Alignment of Single-Photon Emitters in Diamond using Strain Gradient." Physical Review Applied **10**(2): 024050.